

How to mesh up Ewald sums. II. An accurate error estimate for the particle–particle–particle-mesh algorithm

Markus Deserno and Christian Holm

Max-Planck-Institut für Polymerforschung, Ackermannweg 10, 55128 Mainz, Germany

(Received 23 June 1998; accepted 6 August 1998)

We construct an accurate estimate for the root mean square force error of the particle–particle–particle mesh (P³M) algorithm by extending a single particle pair error measure which has been given by Hockney and Eastwood. We also derive an easy to use analytic approximation to the error formula. This allows a straightforward and precise determination of the optimal splitting parameter (as a function of system specifications and P³M parameters) and hence knowledge of the force accuracy prior to the actual simulation. The high quality of the estimate is demonstrated in several examples. © 1998 American Institute of Physics. [S0021-9606(98)51642-X]

INTRODUCTION

The combination of periodic boundary conditions and long range interactions is a frequent difficulty encountered in computer simulations of physical systems, and the ingenious summation technique connected with the name of Ewald¹ has become a standard instrument for tackling this problem. However, it has long been realized that for rather extensive simulations (involving, e.g., many particles) this approach is still too time consuming and various alternative methods have been invented. One particular class of these new algorithms owes its speedup to an inspired replacement of the Fourier transformation — which lies at the heart of the Ewald technique — by fast Fourier transform (FFT) routines.^{2–4}

In paper I on mesh based Ewald sums⁵ we presented a unified view of these FFT accelerated methods and carried out detailed accuracy measurements. However, since all these algorithms contain various free parameters, working at the maximally obtainable accuracy requires the user to tune them very carefully. This is straightforward if there exists a theoretical estimate of the errors involved — as is the case for the standard Ewald sum⁶ as well as for the so-called particle mesh Ewald (PME) method⁷ — but rather tedious otherwise.

In this paper we present such an estimate for the root mean square error in the force of the so-called particle–particle–particle mesh (P³M) algorithm by extending an error measure already derived by Hockney and Eastwood² and additionally provide an easy to use analytical approximation to the somewhat unwieldy expression comprising various sums.

EWALD SUM AND P³M IN A NUTSHELL

In this section we outline for reference purposes the most important formulas for the P³M method without much explanation, derivation or motivation. For details the reader is referred to the original P³M literature² as well as paper I.

Consider a system of N particles with charges q_i at positions \mathbf{r}_i in an overall neutral cubic simulation box of length

L . Employing the Ewald sum, the force \mathbf{F}_i on particle i , which results from all interactions with the other charges (including all periodic images), can be written in the following way:

$$\mathbf{F}_i = \mathbf{F}_i^{(r)} + \mathbf{F}_i^{(k)} + \mathbf{F}_i^{(d)}. \quad (1)$$

The so-called real space, Fourier space and dipole contributions are, respectively, given by

$$\begin{aligned} \mathbf{F}_i^{(r)} = q_i \sum_j q_j \sum_{\mathbf{m} \in \mathbb{Z}^3} \left(\frac{2\alpha}{\sqrt{\pi}} \exp(-\alpha^2 |\mathbf{r}_{ij} + \mathbf{m}L|^2) \right. \\ \left. + \frac{\operatorname{erfc}(\alpha |\mathbf{r}_{ij} + \mathbf{m}L|)}{|\mathbf{r}_{ij} + \mathbf{m}L|} \right) \frac{\mathbf{r}_{ij} + \mathbf{m}L}{|\mathbf{r}_{ij} + \mathbf{m}L|^2}, \end{aligned} \quad (2)$$

$$\mathbf{F}_i^{(k)} = \frac{q_i}{L^3} \sum_j q_j \sum_{\mathbf{k} \neq 0} \frac{4\pi\mathbf{k}}{k^2} \exp\left(-\frac{k^2}{4\alpha^2}\right) \sin(\mathbf{k} \cdot \mathbf{r}_{ij}), \quad (3)$$

$$\mathbf{F}_i^{(d)} = -\frac{4\pi q_i}{(1+2\epsilon')L^3} \sum_j q_j \mathbf{r}_j. \quad (4)$$

The prime on the second sum in Eq. (2) indicates that for $i=j$ the term $\mathbf{m}=0$ has to be omitted, $\operatorname{erfc}(r) := 2\pi^{-1/2} \int_r^\infty dt \exp(-t^2)$ is the complementary error function and of course $\mathbf{r}_{ij} = \mathbf{r}_i - \mathbf{r}_j$. Furthermore, the inverse length α is the *splitting parameter* of the Ewald sum, which controls the relative importance of the contributions coming from real and reciprocal space, the \mathbf{k} -vectors are from the discrete set $(2\pi/L)\mathbb{Z}^3$ and ϵ' is the dielectric constant of the medium, which surrounds the cluster of simulation boxes as it tends (in a spherical way) toward an infinite system. In practice, the infinite sums in Eqs. (2) and (3) are truncated by only taking into account distances which are smaller than some real space cutoff r_{\max} and wave vectors with a modulus smaller than some reciprocal space cutoff k_{\max} .

The P³M method offers a fast way for an approximate computation of the reciprocal space contribution (3). By mapping the system onto a mesh, the necessary Fourier

transformations can be accomplished by fast Fourier routines. At the same time the simple Coulomb Green function $4\pi/k^2$ is adjusted as to make the result of the mesh calculation most closely resemble the continuum solution.

The first step, i.e., generating the mesh based charge density ρ_M (defined at the mesh points \mathbf{r}_p), is carried out with the help of a charge assignment function W :

$$\rho_M(\mathbf{r}_p) = \frac{1}{h^3} \sum_{i=1}^N q_i W(\mathbf{r}_p - \mathbf{r}_i). \quad (5)$$

Here h is the mesh spacing, and the number of mesh points $N_M = L/h$ along each direction should preferably be a power of two, since in this case the FFT is most efficient. The charge assignment function is classified according to its order P , i.e., between how many grid points — per coordinate direction — each charge is distributed. In the P³M method introduced by Hockney and Eastwood² its Fourier transform is

$$\tilde{W}(\mathbf{k}) = h^3 \left(\frac{\sin\left(\frac{1}{2}k_x h\right) \sin\left(\frac{1}{2}k_y h\right) \sin\left(\frac{1}{2}k_z h\right)}{\frac{1}{2}k_x h \frac{1}{2}k_y h \frac{1}{2}k_z h} \right)^P. \quad (6)$$

In a second step the mesh based electric field $\mathbf{E}(\mathbf{r}_p)$ is calculated. Basically, the electric field is the derivative of the electrostatic potential, but there exist several alternatives for implementing the differentiation on a lattice.⁵ In this paper we will restrict ourselves to the case of *ik-differentiation*, which works by multiplying the Fourier transformed potential with $i\mathbf{k}$. In this case $\mathbf{E}(\mathbf{r}_p)$ can be written as

$$\mathbf{E}(\mathbf{r}_p) = \text{FFT}[-i\mathbf{k} \times \text{FFT}[\rho_M] \times \hat{G}_{\text{opt}}](\mathbf{r}_p). \quad (7)$$

In other words, $\mathbf{E}(\mathbf{r}_p)$ is the *backward* finite Fourier transform of the product of $-i\mathbf{k}$, the *forward* finite Fourier transform of the mesh based charge density ρ_M and the so-called optimal influence function \hat{G}_{opt} , given by

$$\hat{G}_{\text{opt}}(\mathbf{k}) = \frac{\tilde{\mathbf{D}}(\mathbf{k}) \cdot \sum_{\mathbf{m} \in \mathbb{Z}^3} \tilde{U}^2\left(\mathbf{k} + \frac{2\pi}{h}\mathbf{m}\right) \tilde{\mathbf{R}}\left(\mathbf{k} + \frac{2\pi}{h}\mathbf{m}\right)}{|\tilde{\mathbf{D}}(\mathbf{k})|^2 \left[\sum_{\mathbf{m} \in \mathbb{Z}^3} \tilde{U}^2\left(\mathbf{k} + \frac{2\pi}{h}\mathbf{m}\right) \right]^2}, \quad (8)$$

with

$$\tilde{\mathbf{R}}(\mathbf{k}) := -i\mathbf{k} \frac{4\pi}{k^2} e^{-k^2/4\alpha^2} \quad (9)$$

and

$$\tilde{U}(\mathbf{k}) := \tilde{W}(\mathbf{k})/h^3. \quad (10)$$

Here $\tilde{\mathbf{D}}(\mathbf{k})$ is the Fourier transform of the employed differentiation operator, which is simply $i\mathbf{k}$ in our case. Finally, one arrives at the force on particle i , i.e., the replacement of Eq. (3):

$$\mathbf{F}_i = q_i \sum_{\mathbf{r}_p \in \mathbb{M}} \mathbf{E}(\mathbf{r}_p) W(\mathbf{r}_i - \mathbf{r}_p). \quad (11)$$

Hereby the sum extends over the complete mesh \mathbb{M} .

Although the presented formulas (5)–(11) look somewhat complicated, it is rather easy to implement them step by step. Furthermore, due to the replacement of the Fourier transforms by FFT routines [see Eq. (7)], the algorithm is not only fast but its CPU time shows a favorable scaling with particle number: If the real space cutoff r_{max} is chosen small enough [so that the real space contribution (2) can be calculated in order N], the complete algorithm is essentially of order $N \log N$.

SCALING OF THE rms FORCE ERROR

In this section we address the dependence of the root mean square error in the force on the number of charged particles and their valence. Since the assumptions and arguments involved are of a rather general nature, the result is not specific to a certain kind of Ewald method.

We define the rms error in the force to be

$$\Delta F := \sqrt{\frac{1}{N} \sum_{i=1}^N (\mathbf{F}_i - \mathbf{F}_i^{\text{exa}})^2} =: \sqrt{\frac{1}{N} \sum_{i=1}^N (\Delta \mathbf{F}_i)^2}, \quad (12)$$

where \mathbf{F}_i is the force on particle i calculated by the algorithm under investigation and $\mathbf{F}_i^{\text{exa}}$ is the *exact* force on that particle. Note that this is by no means the only interesting measure of accuracy. However, it is the only one which is considered in this paper.

We now assume that the error in the force on particle i can be written as

$$\Delta \mathbf{F}_i = q_i \sum_{j \neq i} q_j \chi_{ij}. \quad (13)$$

The idea behind this ansatz is that — just as it is true for \mathbf{F}_i — the *error* in \mathbf{F}_i originates from the $N-1$ interactions of particle i with the other charged particles, and each contribution should be proportional to the product of the two charges involved. The vector χ_{ij} gives the direction and magnitude of this error for two unit charges and depends on their separation and orientation as well as on the specific algorithm used for calculating the electrostatic forces. For this term we further assume

$$\langle \chi_{ij} \cdot \chi_{ik} \rangle = \delta_{jk} \langle \chi_{ij}^2 \rangle =: \delta_{jk} \chi^2, \quad (14)$$

where averaging over the particle configurations is denoted by the angular brackets. The underlying assumption that contributions from different particles are uncorrelated is certainly not always true (think, e.g., of highly ordered or strongly inhomogeneous particle distributions), but it is sensible for *random* systems. Obviously, the term $\langle \chi_{ij}^2 \rangle$ — the mean square force error for two unit charges — can no longer depend on i and j and is thus written as χ^2 . Using Eqs. (13) and (14), it follows

$$\langle (\Delta \mathbf{F}_i)^2 \rangle = q_i^2 \sum_{j \neq i} \sum_{k \neq i} q_j q_k \langle \chi_{ij} \cdot \chi_{ik} \rangle \approx q_i^2 \chi^2 Q^2 \quad (15)$$

where the important quantity Q^2 is defined as

$$Q^2 := \sum_{j=1}^N q_j^2. \quad (16)$$

Not all particles necessarily have the same charge. More specifically, let there be P subsets \mathbb{N}_p , defined by the condition that all $|\mathbb{N}_p|$ particles from the subset \mathbb{N}_p have the same charge c_p . If $|\mathbb{N}_p| \gg 1$, the law of large numbers⁸ and Eq. (15) gives

$$\frac{1}{|\mathbb{N}_p|} \sum_{i \in \mathbb{N}_p} (\Delta \mathbf{F}_i)^2 \approx \langle (\Delta \mathbf{F}_i)^2 \rangle_{i \in \mathbb{N}_p} \approx c_p^2 \chi^2 Q^2, \quad (17)$$

i.e., the *arithmetic mean* of the $(\Delta \mathbf{F}_i)^2$ for all particles $i \in \mathbb{N}_p$ can be approximated by the *ensemble average* for one particle from \mathbb{N}_p . In the case where *all* $|\mathbb{N}_p|$ are large, it follows

$$\begin{aligned} \frac{1}{N} \sum_{i=1}^N (\Delta \mathbf{F}_i)^2 &= \sum_{p=1}^P \frac{|\mathbb{N}_p|}{N} \left(\frac{1}{|\mathbb{N}_p|} \sum_{i \in \mathbb{N}_p} (\Delta \mathbf{F}_i)^2 \right) \\ &\approx \chi^2 \frac{Q^2}{N} \sum_{p=1}^P |\mathbb{N}_p| c_p^2 = \chi^2 \frac{Q^4}{N}. \end{aligned} \quad (18)$$

Inserting this into Eq. (12) gives the final relation

$$\Delta F \approx \chi \frac{Q^2}{\sqrt{N}}. \quad (19)$$

Thus, the scaling of the rms error in the force with particle number and valence is given by the factor $Q^2 N^{-1/2}$, whereas the prefactor χ — which cannot be obtained by such simple arguments — contains the details of the method. Indeed, the estimates for the real and reciprocal space error of the standard Ewald sum⁶ as well as the estimate for the reciprocal space error of the PME method⁷ are exactly of the form (19). Note that any information on the valence distribution enters only through the value of Q^2 .

THE ERROR MEASURE OF HOCKNEY AND EASTWOOD

The most interesting ingredient of the P³M method is the optimal influence function from Eq. (8). It is constructed such that the result of the mesh calculation is as close as possible to the solution of the original continuum problem. Of course, this is only realizable in a quantitative way, if the notion of “as close as possible” is stated more precisely. Hockney and Eastwood define the following measure of the error involved in a P³M calculation:

$$Q := \frac{1}{h^3} \int_{h^3} d^3 r_1 \int_{L^3} d^3 r [\mathbf{F}(\mathbf{r}; \mathbf{r}_1) - \mathbf{R}(\mathbf{r})]^2. \quad (20)$$

$\mathbf{F}(\mathbf{r}; \mathbf{r}_1)$ is the Fourier space contribution of the force between two unit charges at positions \mathbf{r}_1 and $\mathbf{r}_1 + \mathbf{r}$ as calculated by the P³M method (note that due to broken rotational and translational symmetry this does in fact depend on the coordinates of *both* particles), and $\mathbf{R}(\mathbf{r})$ is the corresponding exact reference force [whose Fourier transform is just Eq. (9)]. The inner integral over \mathbf{r} scans all particle separations, whereas the outer integral over \mathbf{r}_1 averages over all possible locations of the first particle within a mesh cell. Obviously,

up to a factor L^{-3} this expression is just the mean square error in the force for two unit charges, in other words, the quantity χ^2 from Eq. (14). This provides a link between the rms error of an N particle system and the error Q from Hockney and Eastwood: Using Eq. (19) one obtains

$$\Delta F \approx Q^2 \sqrt{\frac{Q}{NL^3}}. \quad (21)$$

Technically spoken, Q is a *functional* of the influence function, and by setting the functional derivative of Q with respect to \hat{G} to zero Hockney and Eastwood were able to derive the optimal influence function from Eq. (8). However, it is most important to realize that they also provide a closed expression for the corresponding “optimal error” $Q_{\text{opt}} = Q[\hat{G}_{\text{opt}}]$:

$$\begin{aligned} Q_{\text{opt}} &= \frac{1}{L^3} \sum_{\mathbf{k} \in \hat{\mathbb{M}}} \left\{ \sum_{\mathbf{m} \in \mathbb{Z}^3} \left| \tilde{\mathbf{R}} \left(\mathbf{k} + \frac{2\pi}{h} \mathbf{m} \right) \right|^2 \right. \\ &\quad \left. - \frac{\left| \tilde{\mathbf{D}}(\mathbf{k}) \cdot \sum_{\mathbf{m} \in \mathbb{Z}^3} \tilde{U}^2 \left(\mathbf{k} + \frac{2\pi}{h} \mathbf{m} \right) \tilde{\mathbf{R}}^* \left(\mathbf{k} + \frac{2\pi}{h} \mathbf{m} \right) \right|^2}{|\tilde{\mathbf{D}}(\mathbf{k})|^2 \left[\sum_{\mathbf{m} \in \mathbb{Z}^3} \tilde{U}^2 \left(\mathbf{k} + \frac{2\pi}{h} \mathbf{m} \right) \right]^2} \right\}. \end{aligned} \quad (22)$$

The outer sum extends over all \mathbf{k} -vectors of the Fourier transformed mesh $\hat{\mathbb{M}}$, and the star denotes complex conjugation. Once again, in the special case of $i\mathbf{k}$ -differentiation one has $\tilde{\mathbf{D}}(\mathbf{k}) = i\mathbf{k}$.

Admittedly, Eq. (22) looks rather complicated. Still, in combination with Eq. (21) it gives the rms force error of the P³M method (or — more precisely — of its Fourier space contribution)! (After all, the computation of Q_{opt} and that of \hat{G}_{opt} are quite similar.) We would like to emphasize that the formula (22) for the optimal Q value [just like the one for the optimal influence function (8)] is of a very general nature: It does also work for different charge assignment functions, reference forces or any differentiation scheme which can be expressed by an operator $\tilde{\mathbf{D}}(\mathbf{k})$, in particular for all the finite difference schemes presented in paper I.

The corresponding rms error in the force from the real space contribution (2) has been derived by Kolafa and Perram⁶ and we want to provide it here for reference purposes:

$$\Delta F^{(r)} \approx \frac{2Q^2}{\sqrt{N} r_{\text{max}} L^3} \exp(-\alpha^2 r_{\text{max}}^2). \quad (23)$$

With these two estimates at hand it is easy to determine the optimal value of the splitting parameter α via a stand-alone program, which takes the relevant system parameters (N , Q^2 , L) and specifications of the algorithm (r_{max} , N_M , P) as its input. If real and reciprocal space contribution to the error, $\Delta F^{(r)}$ and $\Delta F^{(k)}$, respectively, are assumed to be statistically independent, the total error is given by

TABLE I. Expansion coefficients $c_m^{(P)}$ for the functions $f^{(P)}$ from Eqs. (26) and (29) as needed in Eq. (30).

P	$c_0^{(P)}$	$c_1^{(P)}$	$c_2^{(P)}$	$c_3^{(P)}$	$c_4^{(P)}$	$c_5^{(P)}$	$c_6^{(P)}$
1	$\frac{2}{3}$						
2	$\frac{2}{45}$	$\frac{8}{189}$					
3	$\frac{4}{945}$	$\frac{2}{225}$	$\frac{8}{1485}$				
4	$\frac{2}{4725}$	$\frac{16}{10395}$	$\frac{5528}{3869775}$	$\frac{32}{42525}$			
5	$\frac{4}{93555}$	$\frac{2764}{11609325}$	$\frac{8}{25515}$	$\frac{7234}{32531625}$	$\frac{350936}{3206852775}$		
6	$\frac{2764}{638512875}$	$\frac{16}{467775}$	$\frac{7234}{119282625}$	$\frac{1403744}{25196700375}$	$\frac{1396888}{40521009375}$	$\frac{2485856}{152506344375}$	
7	$\frac{8}{18243225}$	$\frac{7234}{1550674125}$	$\frac{701872}{65511420975}$	$\frac{2793776}{225759909375}$	$\frac{1242928}{132172165125}$	$\frac{1890912728}{352985880121875}$	$\frac{21053792}{8533724574375}$

$$\Delta F = \sqrt{(\Delta F^{(r)})^2 + (\Delta F^{(k)})^2}. \quad (24)$$

This quantity has to be minimized with respect to α . However, in most cases it is accurate enough to use the following approximation: Determine the value of α at which the real and reciprocal space contribution to the rms force error are equal.

ANALYTIC APPROXIMATION

Although the closed expression for the error from the last section is not really *complicated*, it is somewhat *unwieldy*. A possible calculation of the optimal value of α using, e.g., a bisection method needs several computations of Q_{opt} and for each it is necessary to compute the inner aliasing sums and the outer sum over the \mathbf{k} -vectors. Especially for large Fourier meshes this can be rather time consuming. Therefore we now derive an analytic approximation to this error estimate, which is essentially an *expansion for small* $h\alpha$. We will restrict ourselves to the case of a cubic system and the same number N_M of mesh points along each direction. Also, we will only treat the case of $i\mathbf{k}$ -differentiation [see Eq. (7)], since we found⁵ that this is the most accurate method. However, our line of reasoning can be extended to more general cases.

We start our treatment of Eq. (22) by observing that two of the three sums over \mathbb{Z}^3 contain $\tilde{\mathbf{R}}$ with its exponential factor $\exp(-k^2/4\alpha^2)$. Since near the boundary of $\hat{\mathbb{M}}$ its value is roughly given by $\exp(-(\pi/h\alpha)^2)$, $\tilde{\mathbf{R}}$ is strongly damped outside $\hat{\mathbb{M}}$ if $h\alpha$ is small. Thus, it is a good approximation to retain only the term with $\mathbf{m}=0$ in these two sums. Inserting $\tilde{\mathbf{D}}(\mathbf{k})=i\mathbf{k}$, the Fourier transform of the charge assignment function from Eq. (5) and using the fact that $\sin^2(x+n\pi)=\sin^2(x)$ for integral n , one obtains

$$Q_{\text{opt}} \approx \frac{(4\pi)^2}{L^3} \sum_{\mathbf{k} \in \hat{\mathbb{M}}} \frac{e^{-k^2/2\alpha^2}}{k^2} \times \left\{ 1 - f^{(P)}\left(\frac{k_x h}{2}\right) f^{(P)}\left(\frac{k_y h}{2}\right) f^{(P)}\left(\frac{k_z h}{2}\right) \right\} \quad (25)$$

with the function $f^{(P)}$ defined as

$$f^{(P)}(x) := \frac{x^{-4P}}{\left(\sum_{m \in \mathbb{Z}} (x+m\pi)^{-2P} \right)^2}. \quad (26)$$

In a second step the aliasing sum in the denominator of Eq. (26) is evaluated analytically by exploiting the following partial fraction expansion:⁹

$$\sin^{-2}(x) = \sum_{m \in \mathbb{Z}} (x+m\pi)^{-2}, \quad x \in \mathbb{R} \setminus \pi\mathbb{Z}. \quad (27)$$

Differentiating this expression $2P-2$ times gives

$$\sum_{m \in \mathbb{Z}} (x+m\pi)^{-2P} = \frac{1}{(2P-1)!} \frac{d^{2P-2}}{dx^{2P-2}} \sin^{-2}(x). \quad (28)$$

This equation leads to a closed expression for the function $f^{(P)}$ from Eq. (26):

$$f^{(P)}(x) = \frac{[(2P-1)!]^2}{x^{4P}} \left(\frac{d^{2P-2}}{dx^{2P-2}} \sin^{-2}(x) \right)^{-2}. \quad (29)$$

Unfortunately the sum over $\hat{\mathbb{M}}$ is still too complicated to perform, so some further approximations are necessary. We choose the following way: $f^{(P)}$ is expanded in a Taylor series up to order $4P-2$. Since (i) $f^{(P)}$ is an even function, (ii) $f^{(P)}(0)=1$ and (iii) the lowest nontrivial term is of order x^{2P} , this expansion can be written as

$$f^{(P)}(x) \approx f_T^{(P)}(x) := 1 - x^{2P} \sum_{m=0}^{P-1} c_m^{(P)} x^{2m}. \quad (30)$$

The coefficients $c_m^{(P)}$ are easily determined with the help of any mathematical computer program capable of symbolic algebra and are listed in Table I. The term in curly brackets from Eq. (25) can now be approximated as follows:

TABLE II. Expansion coefficients $a_m^{(P)}$ from Eq. (37).

P	$a_0^{(P)}$	$a_1^{(P)}$	$a_2^{(P)}$	$a_3^{(P)}$	$a_4^{(P)}$	$a_5^{(P)}$	$a_6^{(P)}$
1	$\frac{2}{3}$						
2	$\frac{1}{50}$	$\frac{5}{294}$					
3	$\frac{1}{588}$	$\frac{7}{1440}$	$\frac{21}{3872}$				
4	$\frac{1}{4320}$	$\frac{3}{1936}$	$\frac{7601}{2\,271\,360}$	$\frac{143}{28\,800}$			
5	$\frac{1}{23\,232}$	$\frac{7601}{13\,628\,160}$	$\frac{143}{69\,120}$	$\frac{517\,231}{106\,536\,960}$	$\frac{106\,640\,677}{11\,737\,571\,328}$		
6	$\frac{691}{68\,140\,800}$	$\frac{13}{57\,600}$	$\frac{47\,021}{35\,512\,320}$	$\frac{9\,694\,607}{2\,095\,994\,880}$	$\frac{733\,191\,589}{59\,609\,088\,000}$	$\frac{326\,190\,917}{11\,700\,633\,600}$	
7	$\frac{1}{345\,600}$	$\frac{3617}{35\,512\,320}$	$\frac{745\,739}{838\,397\,952}$	$\frac{56\,399\,353}{12\,773\,376\,000}$	$\frac{25\,091\,609}{1\,560\,084\,480}$	$\frac{1\,755\,948\,832\,039}{36\,229\,939\,200\,000}$	$\frac{4\,887\,769\,399}{37\,838\,389\,248}$

$$1 - f^{(P)}\left(\frac{k_x h}{2}\right) f^{(P)}\left(\frac{k_y h}{2}\right) f^{(P)}\left(\frac{k_z h}{2}\right) \\ \approx \left(1 - f_T^{(P)}\left(\frac{k_x h}{2}\right)\right) + \left(1 - f_T^{(P)}\left(\frac{k_y h}{2}\right)\right) + \left(1 - f_T^{(P)}\left(\frac{k_z h}{2}\right)\right). \quad (31)$$

The product of the three functions $f^{(P)}$ is computed by multiplying their Taylor expansions term by term, but the results are only retained up to the truncation order $4P-2$. Note that the first neglected cross term would be of order $4P$.

For symmetry reasons it is clear that all three terms in the last line of Eq. (31) contribute in the same way to the value of the sum in Eq. (25), therefore it suffices to choose one of them, e.g., the z term, and multiply the result by 3. Together with the definition of $f_T^{(P)}$ from Eq. (30) this leads to

$$Q_{\text{opt}} \approx 3 \frac{(4\pi)^2}{L^3} \sum_{\mathbf{k} \in \hat{\mathbb{M}}} \frac{e^{-k^2/2\alpha^2 P-1}}{k^2} \sum_{m=0} c_m^{(P)} \left(\frac{k_z h}{2}\right)^{2(P+m)}. \quad (32)$$

Finally, the sum is replaced by an integral via

$$\left(\frac{2\pi}{L}\right)^3 \sum_{\mathbf{k}} \rightarrow \int d^3k. \quad (33)$$

If one extends the range of integration to \mathbb{R}^3 and changes to spherical polar coordinates, the remaining angular and radial integrals can be performed with the help of

$$\int_0^\pi d\vartheta \sin \vartheta \cos^{2n} \vartheta = \frac{2}{2n+1}, \quad n \in \mathbb{N} \quad (34)$$

and

$$\int_0^\infty dx x^{2n} e^{-x^2} = \frac{\sqrt{\pi} (2n-1)!!}{2^{n+1}}, \quad n \in \mathbb{N} \quad (35)$$

where $(2n-1)!! = 1 \cdot 3 \cdot 5 \cdots (2n-1)$. Collecting all parts together gives

$$Q_{\text{opt}} \approx \sqrt{2\pi} \alpha (h\alpha)^{2P} \sum_{m=0}^{P-1} a_m^{(P)} (h\alpha)^{2m} \quad (36)$$

with the abbreviation

$$a_m^{(P)} := 12 \frac{(2(P+m)-1)!!}{2(P+m)+1} 2^{-2(P+m)} c_m^{(P)}. \quad (37)$$

Combining this with Eq. (21) results in the following analytical approximation to the Fourier space contribution to the rms force error of the P³M algorithm:

$$\Delta F \approx \frac{Q^2}{L^2} (h\alpha)^P \sqrt{\frac{\alpha L}{N} \sqrt{2\pi} \sum_{m=0}^{P-1} a_m^{(P)} (h\alpha)^{2m}}. \quad (38)$$

The exact expansion coefficients $a_m^{(P)}$ (which are rational numbers) are listed in Table II.

Let us repeat that Eq. (38) was derived under the explicit assumption that $h\alpha$ is small. Both, the restriction to the term $\mathbf{m}=0$ for two sums in Eq. (22) as well as the expansion of the function $f^{(P)}$ from Eqs. (26) and (29) in powers of $h\alpha$ can become questionable if $h\alpha$ becomes large. However, in this case it is still safe to go back to the original error estimate, i.e., the combination of Eqs. (21) and (22).

NUMERICAL TEST

In this section we demonstrate the accuracy of the P³M error estimates by comparing their predictions with the exact rms force error ΔF from Eq. (12) — calculated for a specific random system. Hereby the exact forces \mathbf{F}_i needed for computing ΔF are obtained by a well converged standard Ewald sum, and for the test system we choose the one described in Appendix D of paper I: 100 particles randomly distributed within a cubic box of length $L=10$, half of them carry a positive, the other half a negative unit charge. Our unit conventions are as follows:⁵ lengths are measured in \mathcal{L} and charges in \mathcal{C} . Hence the unit of force is $\mathcal{C}^2/\mathcal{L}^2$. We will

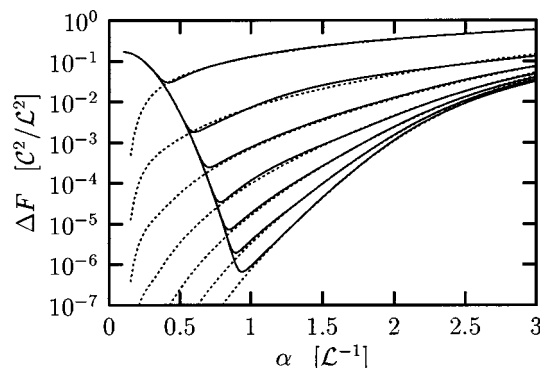


FIG. 1. The rms error ΔF (solid lines) for the system of 100 randomly distributed charges is calculated for the $i\mathbf{k}$ -differentiated P³M method with $N_M=32$ mesh points and real space cutoff $r_{\max}=4$. From top to bottom the order of the charge assignment function is increased from 1 to 7. The dotted lines are the corresponding full estimates [using Eqs. (21) and (22)] for the Fourier space contribution to ΔF .

refer to the estimate which emerges from combining Eqs. (21) and (22) as the *full estimate* and to Eq. (38) as the *analytical approximation*.

In a first example we fix the number of mesh points to $N_M=32$ and the real space cutoff to $r_{\max}=4$. The charge assignment order varies from $P=1$ through $P=7$. In Fig. 1 the resulting curves for the rms force error ΔF are plotted together with the full error estimate and in Fig. 2 the same is done for the analytical approximation. It can be seen very clearly that the full estimate accurately predicts the Fourier space contribution to ΔF for all values of α and P . Since the real space contribution is also known⁶ [see also Eq. (23)], this permits an easy determination of the optimal value of the splitting parameter α . The analytical approximation is almost as accurate as the full formula, however, for large P it diminishes in accuracy if α gets large. This is due to the fact that Eq. (38) was derived under the assumption that $h\alpha$ is small. Note that the expansion coefficients $a_m^{(P)}$ needed in Eq. (38) strongly increase with increasing m if P gets larger (see Table II). Still, both estimates are useful for determining the optimal operation point, and Eq. (38) can be calculated much faster than the sums from Eq. (22).

Next we study at fixed charge assignment order $P=3$ different mesh sizes $h=L/N_M$ by investigating N_M

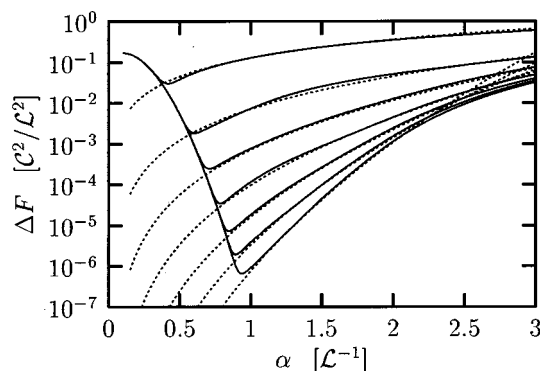


FIG. 2. The same plot as in Fig. 1, but here the dotted lines are the analytical estimates from Eq. (38). Note that for large P the error ΔF is overestimated at large values of α .

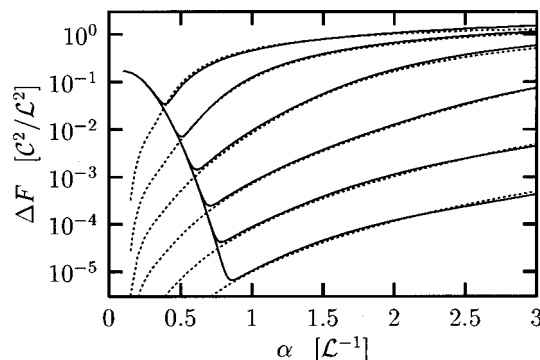


FIG. 3. ΔF (solid lines) for the same system as in the previous figures is calculated for the $i\mathbf{k}$ -differentiated P³M method with charge assignment order $P=3$ and real space cutoff $r_{\max}=4$. From top to bottom the number of mesh points varies like 4, 8, 16, 32, 64, 128. The dotted lines are the corresponding full error estimates.

$\in\{4,8,16,32,64,128\}$. Figures 3 and 4 show ΔF in comparison with the full and the approximated error estimate, respectively. Again, it can be seen that the former very accurately gives the Fourier space contribution to ΔF . As expected, the analytical approximation has problems at small N_M (since this results in large h), but nevertheless it is very useful otherwise. Essentially, one has to check the value of $h\alpha$: If this is of the order unity or even larger, care is called for. Note that in Fig. 4 the value of $h\alpha$ is approximately 1 at the points where the analytical approximation starts to deviate from the true curve.

In a next step we want to demonstrate that the scaling of the rms force error with particle number and valence distribution is in fact correctly given by $\Delta F \propto Q^2 N^{-1/2}$. To this end we investigate three systems which differ *only* in the values of Q^2 and N . The first system is the same as the one investigated so far in Figs. 1–4. A second system contains 200 particles, namely, 50 monovalent and 50 trivalent pairs. Finally, a third system contains 400 particles: 50 pairs with charge ± 1 , 100 pairs with charge ± 5 and 50 pairs with charge ± 7 . Hence, their (Q^2, N) values are, respectively, given by (100,100), (1000,200) and (10 000,400), and the ratio of their scaling prefactors is thus $1:\sqrt{50}:50$. In Fig. 5 this is clearly visible in the constant shift of the three curves with respect to one another (note that the vertical scale is

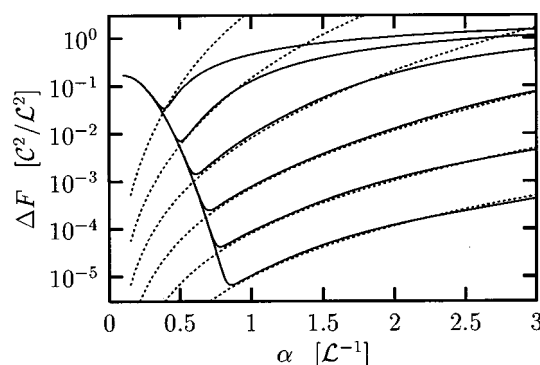


FIG. 4. The same plot as in Fig. 3, but here the dotted lines are the analytical estimates from Eq. (38). At small N_M , which corresponds to large values of $h=L/N_M$, the error formula overestimates ΔF at large values of α .

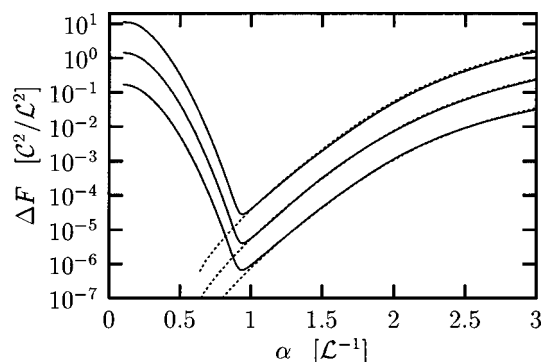


FIG. 5. Test of the $Q^2 N^{-1/2}$ scaling of ΔF . The three solid lines show the rms force error ΔF for systems, which differ in their (Q^2, N) values. From top to bottom they are characterized by (10 000, 400), (1000, 200) and (100, 100) (the last system is the same as the one in Figs. 1–4). The dotted curves are the corresponding full error estimates.

logarithmic). Also shown is the full error estimate, which again predicts the Fourier space contribution to ΔF in all three cases very precisely.

APPLICATION TO AN INHOMOGENEOUS POLYELECTROLYTE SYSTEM

So far we have only used homogeneous random systems for testing the error estimates. However, this does not necessarily reflect the situation encountered in all computer experiments. In the present section we want to show that deviations from a random distribution, as they frequently occur in charged systems, in fact have a noticeable influence on the rms error.

We will use a typical system from our own research to demonstrate this effect: a simple model of a polyelectrolyte solution.^{10,11} 106 Lennard–Jones particles were joined (by some bonding potential) to build up a polymer chain. Every third “monomer” was monovalently charged and 8 such chains together with 96 trivalent and oppositely charged counterions, which make the complete system electrically neutral, were put in a cubic simulation box of length $L \approx 179$. The system was brought into the canonical state by means of a molecular dynamics simulation and a Langevin thermostat.

Under certain circumstances (e.g., at sufficiently low temperature and the appropriate density range) such polyelectrolyte chains collapse, and this happened to the described system. The chain sizes shrunk to much smaller values than for comparable neutral polymers and 90% of the counterions were condensed within a distance of only two Lennard–Jones radii from the nearest chain.

The various phenomena leading to this transition, the influence of the system parameters or the dynamics are only a few of the interesting physical questions. However, the only thing which concerns us here is the fact that after the transition the system has developed local inhomogeneities. To demonstrate this we have plotted in Fig. 6 the measured relative frequency $p(r/L)$ of the scaled *minimum image distance* $r/L \in [0; \sqrt{3}/2]$ between two charges (we did not distinguish between different valences) and compared this to the probability density of r/L for a random system. The dif-

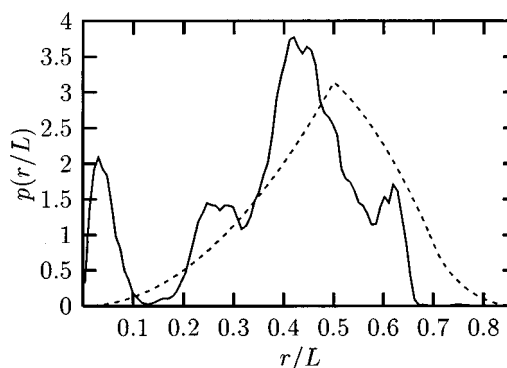


FIG. 6. Measured relative frequency $p(r/L)$ for the scaled minimum image separation r/L between two charges of the polyelectrolyte system described in the text (the solid line). For comparison, the probability density of r/L for a random system is also shown (the dashed line).

ferences are indeed very pronounced. Apart from the more complicated structure of the measured curve, note in particular that small separations are more frequent at the expense of larger ones.

For this system we calculated the rms force error ΔF and the corresponding estimates for the real and reciprocal space contribution [Eqs. (23), (21), (22)]. Since the simulation box comprises 288 monovalent and 96 trivalent charges, we have $N=384$ and $Q=1152$. The result is shown in Fig. 7. No longer do the estimates correctly predict the two branches of ΔF . Rather, at small values of α the algorithm gives better results than expected from Eq. (23), while at large values of α the estimated ΔF is smaller than the actual one. However, this trend can be explained qualitatively in the following way: At small values of α the force (and also its error) is dominated by the real space contribution from Eq. (2). This error originates from neglected contributions beyond the real space cutoff r_{\max} . In the case of Fig. 7 we used $r_{\max}/L \approx 0.243$ and from Fig. 6 it can be seen that there are more particles within this cutoff (and thus less beyond) than in the case of a random particle distribution, which should lead to an enhanced real space accuracy. On the other hand, we demonstrated previously (see Fig. 7 of paper I that the

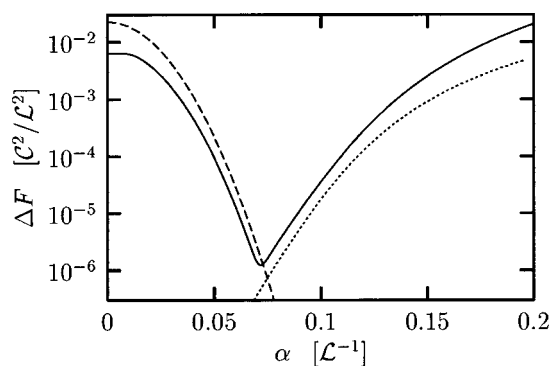


FIG. 7. rms force error ΔF for the polyelectrolyte system described in the text (the solid line). The dotted curve is the full P^3M estimate for the reciprocal space contribution, the dashed curve is the estimate for the real space contribution. Note that due to the strong inhomogeneities in the charge distribution (see Fig. 6) both estimates show systematic deviations from the true error curve.

rms error of the P³M method strongly increases with decreasing minimum image distance. The general shift toward smaller r , which can be observed in the polyelectrolyte system, should thus lead to an enlarged reciprocal space error. Observable effects will occur at large values of α , where this contribution to ΔF dominates.

Although the systematic deviations of the error estimates from the true curve are easily detectable, they are less dramatic than one could have guessed from a brief look at Fig. 6. The optimal splitting parameter from Fig. 7 is given by $\alpha_{\text{opt}} \approx 0.0715$ with a corresponding $\Delta F_{\text{opt}} \approx 1.2 \times 10^{-6}$, while the intersection point of real and reciprocal space estimate occurs at $\alpha \approx 0.0740$, which predicts an error of $\Delta F \approx 9.3 \times 10^{-7}$. If the estimated value of α had been used, this would result in an error of $\Delta F \approx 1.5 \times 10^{-6}$, which is roughly 25% larger than at the optimal value of α . If such a safety margin is considered already at the beginning, the *a priori* determination of the “optimal” value of α by means of Eqs. (21)–(23) together with an *a posteriori* validity check is still a good approach.

In any case, if one knows or at least has reasons to suspect that the investigated system is susceptible to the development of inhomogeneities, one should always be aware of a potential failure of the presented error formulas. In case of doubt, some simple numerical tests — like, e.g., the ones which we have performed here — are neither out of place nor costly.

CONCLUSIONS

We have presented an accurate estimate of the root mean square error in the force involved in a P³M calculation and additionally derived an easy to use analytic approximation for the special case of $i\mathbf{k}$ differentiation. Together with the existing estimate for the real space contribution to the rms force error this permits a determination of the optimal tuning parameter α and provides information on the accuracy which is to be expected. It thus guarantees that one does not waste accuracy which could otherwise be achieved at the same computational effort. Stated the other way around: It prevents one from spending more computational effort for a desired algorithmic accuracy than actually necessary.

In paper I we showed that the $i\mathbf{k}$ -differentiated P³M method is the most accurate algorithm for the FFT accelerated Ewald sum.⁵ In combination with the error estimates this gives a “package” for calculating electrostatic interactions in periodic boundary conditions which is easy to use, very precise, produces known and controllable errors and can thus be optimally tuned in advance. If one wishes to rely on the discrete differentiation operators,⁵ the full error formula (21) and (22) will still work. It is only in the case of the analytic differentiation scheme⁴ that none of the present error estimates is applicable.

As a last point, we stressed several times that the validity of the error estimates is subject to some additional requirements, concerning, e.g., the homogeneity of the system. Nevertheless, it should be obvious that in any case a consultation of the error formulas — perhaps only for a first starting point — is superior to guessing the parameters or the use of α values which were historically handed down. The difficulties of the analytical approximation (38) at large values of $h\alpha$ are not a serious problem anyway, since in case of doubt one can always go back to the full estimate.

ACKNOWLEDGMENTS

Both authors are grateful to K. Kremer for encouragement and helpful comments. C.H. further thanks the DFG for financial support. A large amount of computer time was generously provided by the HLRZ Jülich under Grant No. hkf06.

¹P. Ewald, Ann. Phys. (Leipzig) **64**, 253 (1921).

²R. W. Hockney and J. W. Eastwood, *Computer Simulation Using Particles* (IOP, Bristol, 1988).

³T. Darden, D. York, and L. Pedersen, J. Chem. Phys. **98**, 10089 (1993).

⁴U. Essmann, L. Perera, M. L. Berkowitz, T. Darden, H. Lee, and L. Pedersen, J. Chem. Phys. **103**, 8577 (1995).

⁵M. Deserno and C. Holm, J. Chem. Phys. **109**, 7678 (1998), preceding paper.

⁶J. Kolafa and J. W. Perram, Mol. Simul. **9**, 351 (1992).

⁷H. G. Petersen, J. Chem. Phys. **103**, 3668 (1995).

⁸W. Feller, *An Introduction to Probability Theory and Its Applications*, 2nd ed. (Wiley, New York, 1957).

⁹M. Abramowitz and I. A. Stegun, *Handbook of Mathematical Functions* (Dover, New York, 1970).

¹⁰C. Holm and K. Kremer, in *Proceedings of the 50th Yamada Conference on Polyelectrolytes*, Inuyama, 1998 (in press).

¹¹M. Deserno, C. Holm, K. Kremer, and U. Micka (in preparation).